Measurement of small rotation angles by using a parallel interference pattern

Xiaoli Dai, Osami Sasaki, John E. Greivenkamp, and Takamasa Suzuki

We propose a method for measuring rotation angles by using a parallel interference pattern. At two points on a parallel interference pattern reflected by an object, we detect phase changes in the reflected parallel interference pattern caused by rotations of the object. A high sensitivity, or a high ratio of the phase change to the rotation angle, 17 mrad/arcsec, can be achieved by determining the positions of two detection points. A high spatial resolution of ~0.5 mm is also obtained. We analyze the measurement error caused by the alignment of the parallel interference pattern and a random measurement error caused by the phase detection. The theoretical analyses and the experimental results make the characteristics of the method clear and show that the method has an accuracy of 0.2 arcsec for small rotation angles.

Key words: Angle measurement, parallel interference pattern, interferometry.

1. Introduction

Several optical methods of angle measurement have been described. A method based on the internal reflection effect at an air–glass boundary was proposed.[1] The moiré technique was applied to detect the rotation angles of a grating.[2] Among several methods, methods based on interferometers[3–7] and autocollimators[8] have been widely used in practice. The principle of the methods that use interferometers is the use of two beams that are reflected from two different points on an object and permitted to interfere. The optical path difference between the two beams is then detected to obtain the rotation angle of the object. The measurement sensitivity depends on the distance between the two measuring points on the object. To increase the sensitivity, the distance between the two measuring points must be made larger. The methods that use interferometers have a trade-off between spatial resolution and angular sensitivity, and they are effective for large objects. Autocollimators also are used to measure the angles of large objects. The spatial resolution of an autocollimator must be limited to a few millimeters. This limit is due not only to our ability to bring light through the system but also to diffraction. The system must reimage the point source to a small image size. Excessive diffraction will decrease the angular sensitivity. Therefore that the methods that use interferometers and autocollimators typically have a low spatial resolution cannot be avoided.

We propose a method that uses a parallel interference pattern to measure rotation angles. This parallel interference pattern is reflected by the object, and the phases of the reflected parallel interference pattern are detected at two points. The change in the phase difference between the two phase detection points is a function of the rotation angle of the object. When the object rotates, the phase difference changes. The sensitivity of the method depends on the positions of the two detection points in the reflected parallel interference pattern. We define an equiphase plane as the plane on which the phases of the interference pattern are constant. As the line connecting two detection points becomes parallel to an equiphase plane, the distance along the line between the two points becomes longer and the sensitivity increases. The sensitivity of the method is defined by the ratio of the phase-difference change to the rotation angle. A sensitivity of 17 mrad/arcsec for small rotation angles has been achieved by proper arrangement of the two detection points, A and B. The method has a spatial resolution of ~500 μm, which is an order of the period of the parallel interference pattern. After describing the method's prin-

X. Dai, O. Sasaki, and T. Suzuki are with Niigata University, Niigata 950-21, Japan. X. Dai is with The Graduate School of Science and Technology. O. Sasaki and T. Suzuki are with the Faculty of Engineering. J. E. Greivenkamp is with the Optical Sciences Center, University of Arizona, Tucson, Arizona 85721.

Received 31 October 1994; revised manuscript received 11 April 1995.

0003-6935/95/286380-09$06.00/0.

ciple in Section 2, in Section 3 we analyze value θ_m measured in the nonideal configuration where the equiphase plane and the optical surface are unaligned. In Section 4 we examine two different errors, $\epsilon_{\delta,\phi}$ and ϵ_α, that are caused by the nonideal configuration and random error σ in the detection of the phase difference, respectively. In Section 5 an experimental setup is presented in which a sinusoidal phase-modulating laser diode interferometer with a feedback control system to eliminate fluctuations in the phase of the interference signal is used. This feedback system decreases random error σ greatly. Optical fibers are used for the two detection points in the interference pattern. In Section 6 we show that the experimental results agree well with the theoretical results concerning measurement errors and the measurement range. With the method we measure the small rotation angles of an optical surface with an accuracy of 0.2 arcsec.

2. Principle

When two collimated laser beams intersect with angle γ, a parallel interference pattern occurs. The period of the parallel interference pattern is

$$S = \frac{\lambda}{2\sin(\gamma/2)}, \tag{1}$$

where λ is the wavelength of the laser. We can see alternate dark and bright planes in the interference pattern. The fringes exist everywhere that the two beams overlap. The parallel interference pattern has a phase distribution. The phase of the bright plane is 0 or 2π rad, and the phase of the dark plane is in π radians. We define an equiphase plane as a plane on which the phases of an interference pattern are constant. Figure 1 shows this parallel interference pattern reflected by an optical surface that can rotate around the y axis. The equiphase planes are parallel to the axis of rotation. We refer to the plane perpendicular to the y axis as plane P. For the reflected parallel interference pattern we are interested in the two equiphase planes corresponding to two measurement points whose phases are α_A and α_B.

If the distance d_0 between the two equiphase planes is smaller than period S of the parallel interference pattern, we have

$$d_0 = \frac{\alpha_0}{2\pi} S, \tag{2}$$

where

$$\alpha_0 = |\alpha_A - \alpha_B|. \tag{3}$$

A top view of this arrangement is shown in Fig. 2. Phases α_A and α_B of the two equiphase planes are detected at points A and B, respectively. The line passing points A and B is called a detection line. The angle between the detection line and the line perpendicular to the reflected parallel interference pattern is denoted by β. The value of β is less than $\pi/2$, which means that the value of α_0 is not zero. When the optical surface rotates by a small angle θ, the reflected parallel interference pattern also rotates by an angle 2θ. The sign of angle θ whose rotation direction is shown in Fig. 2 is assumed to be positive. The distance between the two equiphase planes passing the two detection points A and B changes from d_0 to d. The phases of the A and B points change to α_a and α_b, respectively. If d is smaller than S, we have

$$d = \frac{\alpha}{2\pi} S, \tag{4}$$

where

$$\alpha = |\alpha_a - \alpha_b|. \tag{5}$$

On the basis of the geometrical relationship between distances d_0 and d as shown in Fig. 2, we have

$$d = \frac{\cos(\beta - 2\theta)}{\cos\beta} d_0. \tag{6}$$

From Eqs. (2), (4), and (6), α is expressed as

$$\alpha = \frac{\cos(\beta - 2\theta)}{\cos\beta} \alpha_0. \tag{7}$$

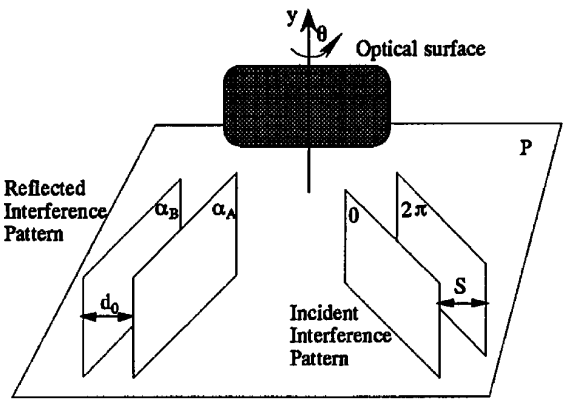

Fig. 1. Parallel interference pattern reflected by an optical surface.

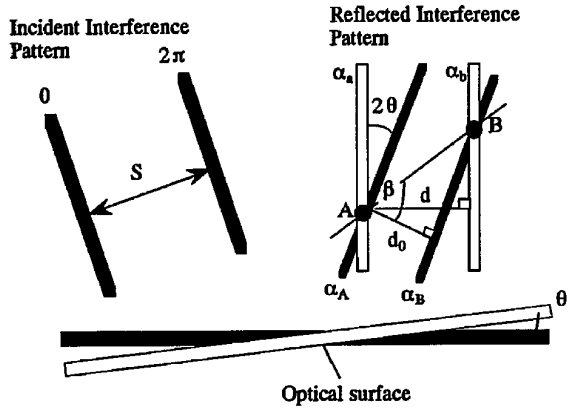

Fig. 2. Fundamental configuration for measuring a rotation angle.

Measuring α_0 and α before and after the rotation of the optical surface, respectively, we can measure the rotation angle θ as follows:

$$\theta = (\beta/2) - (1/2)\cos^{-1}[(\alpha/\alpha_0)\cos(\beta)]. \quad (8)$$

When rotation angle θ is small, Eq. (7) reduces to

$$\alpha \cong (1 + 2\theta \tan \beta)\alpha_0, \quad (9)$$

and we have

$$\theta \cong [(\alpha/\alpha_0) - 1]/2 \tan \beta. \quad (10)$$

We now consider the characteristics of the method. First, the changing ratio of α to θ, or the sensitivity S_e, is obtained from Eq. (7) as follows:

$$S_e = \frac{\partial \alpha}{\partial \theta} = \frac{2 \sin(\beta - 2\theta)}{\cos \beta}\,\alpha_0. \quad (11)$$

The function S_e shows that the sensitivity becomes higher when values of β close to $\pi/2$ and approaching a value of α_0 near 2π are used after the value of β is determined. The value of α_0 becomes close to 2π when the length of the detection line between points A and B is increased or the period S of the incident parallel interference pattern is decreased. The term $\sin(\beta - 2\theta)$ in function S_e indicates that the highest sensitivity exists when the value of angle θ is equal to $\beta/2 - \pi/4$. For the small rotation angle θ, a high sensitivity is obtained when β is nearly equal to $\pi/2$. Therefore this method is especially suitable for measuring small rotation angles. For small rotation angles a high sensitivity of 17 mrad/arcsec is achieved in the conditions of $\beta = 89.9°$ and $\alpha_0 = \pi$ from Eq. (11).

We now consider the measurement range. In Eq. (8) the value of θ is positive when $\alpha > \alpha_0$ and the value of θ is negative when $\alpha < \alpha_0$. This means that we can measure angle θ in two directions of rotation. The maximum and the minimum values of θ arise from the condition of $\alpha = 2\pi$ and $\alpha = 0$, respectively. From Eq. (8) the measurement range of the rotation angle θ is expressed as

$$(\beta/2) - (\pi/4) < \theta < (\beta/2) - (1/2)\cos^{-1}[(2\pi/\alpha_0)\cos \beta]. \quad (12)$$

Using approximation (10), we give the measurement range for small rotation angles by

$$-1/2 \tan \beta < \theta < [(2\pi/\alpha_0) - 1]/2 \tan \beta. \quad (13)$$

When α_0 is equal to π in inequality (13), we have the same measurement range for the positive and negative small rotation angles as follows:

$$|\theta| < 1/2 \tan \beta. \quad (14)$$

It is clear that the measurement range is very small for $\beta \approx \pi/2$. This measurement range refers to a change in tilt between the measurements. A larger measurement range for the system is possible when rotation angle θ is repeatedly monitored. The angular rotation velocity is limited to $1/2 \tan \beta$ per measurement interval.

Finally, this method has a spatial resolution that is an order of period S of the fringe. It is easy to obtain values of S of the order of 500 μm as shown in the experiments. Compared with conventional methods of angle measurements, the spatial resolution in this method is much higher. The highest spatial resolution of an autocollimator is a few millimeters. The spatial resolutions of the methods in which interferometers are used are also a few millimeters when their angular sensitivities are high.

3. Analysis of the Method

With the principle, it is assumed that the equiphase planes and the optical surface are perpendicular to plane P as shown in Fig. 1. This arrangement is ideal. However, in practice it is difficult to adjust the equiphase planes and the optical surface to be absolutely perpendicular to plane P. As shown in Fig. 3 we have two orthogonal coordinate systems, *o–xyz* and *o–x′yz′*, for an equiphase plane and the optical surface, respectively. The *x–z* and *x′–z′* planes are on the P plane. In the ideal configuration the *x′–y* plane is the optical surface and the *y–z* plane is the reflected equiphase plane. The direction of the *z* axis is the propagation direction of the reflected equiphase plane. Because the equiphase plane is incident on the optical surface at angle ω, the angle between the *z* axis and the *z′* axis is ω. Now it is assumed that the incident equiphase planes are inclined toward the P plane by angle δ, and in addition the optical surface is inclined toward the P plane by angle ϕ around the *x′* axis, as shown in Fig. 3. Angles δ, ϕ, and θ whose directions are shown in Fig. 3 are positive. We examine what the measured value θ_m is in this nonideal configuration for the small rotation angle θ.

First, we consider the inclination angle δ of the incident equiphase plane. From the laws of reflection in geometrical optics, it is clear that the inclination of the reflected equiphase plane is also δ. Let

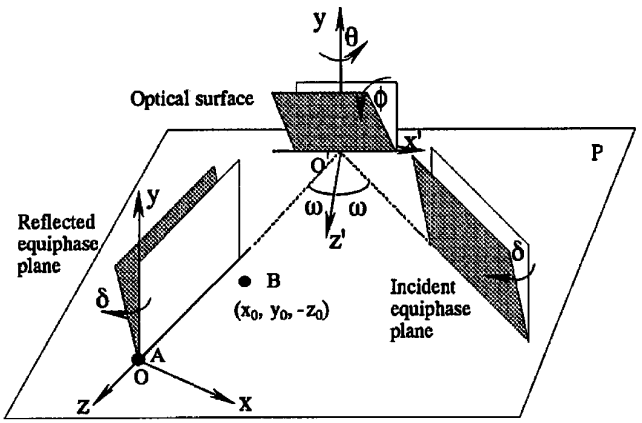

Fig. 3. Nonideal configuration in which the equiphase plane and the optical surface are not perpendicular to plane P.

the normal unit vector of the reflected equiphase plane be $\hat{n}_1$ as shown in Fig. 4(a). If the vectors $\mathbf{n}_{1x}$, $\mathbf{n}_{1y}$, and $\mathbf{n}_{1z}$ are components of the vector $\hat{n}_1$ in the directions of the x, y, and z axes, respectively, the vector $\hat{n}_1$ is given by

$$\hat{n}_1 = (n_{1x}, n_{1y}, n_{1z}), \tag{15}$$

where

$$n_{1x} = \cos\delta, \qquad n_{1y} = \sin\delta, \qquad n_{1z} = 0. \tag{16}$$

To analyze easily how the normal unit vector $\hat{n}_1$ changes with the rotation of the optical surface, the normal unit vector $\hat{n}_1$ is expressed in the o'–$x'yz'$ coordinate system as follows:

$$\hat{n}_1 = (n_{1x'}, n_{1y}, n_{1z'}), \tag{17}$$

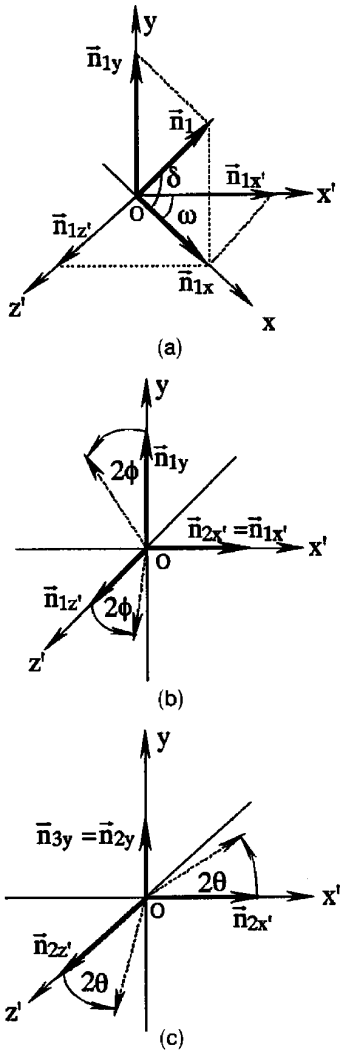

Fig. 4. Change of the normal unit vector of the reflected equiphase plane. (a) Normal unit vector $\hat{n}_1$ in the existence of inclination angle δ of the incident equiphase plane. (b) Rotation of vector $\hat{n}_1$ by inclination angle φ of the optical surface. (c) Rotation of vector $\hat{n}_2$ by rotation angle θ of the optical surface.

where

$$n_{1x'} = \cos\delta\cos\omega, \quad n_{1y} = \sin\delta, \quad n_{1z'} = \cos\delta\sin\omega. \tag{18}$$

Next, when the optical surface inclines toward the P plane by angle φ around the x' axis, the reflected equiphase plane rotates by angle 2φ around the x' axis. This means that vectors $\mathbf{n}_{1y}$ and $\mathbf{n}_{1z'}$ rotate by angle 2φ around the x' axis in the y–z' plane, respectively, and vector $\mathbf{n}_{1x'}$ does not change, as shown in Fig. 4(b). So the normal unit vector $\hat{n}_1$ changes to

$$\hat{n}_2 = (n_{2x'}, n_{2y}, n_{2z'}), \tag{19}$$

where

$$\begin{aligned} &n_{2x'} = n_{1x'}, \qquad n_{2y} = n_{1y}\cos 2\phi - n_{1z'}\sin 2\phi, \\ &n_{2z'} = n_{1y}\sin 2\phi + n_{1z'}\cos 2\phi. \end{aligned} \tag{20}$$

When the optical surface rotates by angle θ around the y axis, the reflected equiphase plane rotates by angle 2θ around the y axis. This means that vectors $\mathbf{n}_{2x'}$ and $\mathbf{n}_{2z'}$ rotate by angle 2θ around the y axis in the x'–z' plane and vector $\mathbf{n}_{2y}$ does not change, as shown in Fig. 4(c). So, the normal unit vector $\hat{n}_2$ changes to

$$\hat{n}_3 = (n_{3x'}, n_{3y}, n_{3z'}), \tag{21}$$

where

$$\begin{aligned} &n_{3x'} = n_{2x'}\cos 2\theta + n_{2z'}\sin 2\theta, \qquad n_{3y} = n_{2y}, \\ &n_{3z'} = -n_{2x'}\sin 2\theta + n_{2z'}\cos 2\theta. \end{aligned} \tag{22}$$

To obtain an expression about the distance d between the two equiphase planes containing detection points A and B, respectively, in the coordinate system o–xyz, it is necessary to obtain an expression of the normal unit vector $\hat{n}_3$ in the coordinate system o–xyz, which is expressed as

$$\hat{n} = (n_x, n_y, n_z). \tag{23}$$

Using a coordinate transformation between the o–xyz and o'–$x'yz'$ coordinate systems, we have

$$\begin{aligned} n_x &= n_{3x'}\cos\omega + n_{3z'}\sin\omega \\ &= n_{2x'}\cos 2\theta\cos\omega + n_{2z'}\cos 2\theta\sin\omega \\ &\quad - n_{2x'}\sin 2\theta\sin\omega + n_{2z'}\sin 2\theta\cos\omega, \end{aligned} \tag{24}$$

$$\begin{aligned} n_z &= n_{3z'}\cos\omega - n_{3x'}\sin\omega \\ &= n_{2z'}\cos 2\theta\cos\omega - n_{2x'}\cos 2\theta\sin\omega \\ &\quad - n_{2x'}\sin 2\theta\cos\omega - n_{2z'}\sin 2\theta\sin\omega, \end{aligned} \tag{25}$$

$$n_y = n_{3y} = n_{2y}. \tag{26}$$

The origin of system o–xyz is point A. Let the coordinates of detection point B be $(x_0, y_0, -z_0)$ in system o–xyz, where $x_0 > 0$, $y_0 > 0$, $z_0 > 0$ and $x_0 \ll$

z_0, $y_0 \ll z_0$. By defining vector **AB** that connects points A and B, we obtain

$$d = \mathbf{n} \cdot \mathbf{AB} = n_x x_0 + n_y y_0 - n_z z_0. \tag{27}$$

When the value of θ is equal to zero in Eqs. (24)–(26), d in Eq. (27) is d_0, which is the distance of the two equiphase planes before the rotation of the optical surface:

$$d_0 = (n_{2x'} \cos \omega + n_{2z'} \sin \omega)x_0 + n_{2y} y_0 - (n_{2z'} \cos \omega - n_{2x'} \sin \omega)z_0. \tag{28}$$

Because this method is very effective for measuring small rotation angles, as shown in the principle, we assume that rotation angle θ is small and use the approximations such as $\sin 2\theta \cong 2\theta$, $\cos 2\theta \cong 1$. Equation (27) reduces to

$$d = d_0 + 2\theta[(-n_{2x'} \sin \omega + n_{2z'} \cos \omega)x_0 + (n_{2x'} \cos \omega + n_{2z'} \sin \omega)z_0]. \tag{29}$$

Using Eqs. (18) and (20), we reduce Eq. (29) to

$$d - d_0 = 2\theta z_0[\cos \delta + 2 \sin \phi[(x_0/z_0)\cos \omega + \sin \omega] \times (\sin \delta \cos \phi - \cos \delta \sin \phi \sin \omega)]. \tag{30}$$

Comparing Figs. 2 and 3, in the ideal configuration we have

$$d_0 = x_0, \qquad \tan \beta = z_0/x_0. \tag{31}$$

From Eqs. (2), (4), and (31), Eq. (10) is rewritten as

$$\theta = \frac{d - d_0}{2z_0}. \tag{32}$$

It is clear from Eqs. (30) and (32) that there is no error caused by the condition where the two points A and B are not on the x–z plane. This property makes it easy to obtain a very small x_0 or d_0 in the experiment. We obtain value θ_m measured in the nonideal configuration for an actual small rotation angle θ by using Eq. (32). Substituting Eq. (30) into Eq. (32), we have

$$\theta_m = K\theta, \tag{33}$$

where

$$K = \cos \delta + 2 \sin \phi[(\cos \omega/\tan \beta) + \sin \omega] \times (\sin \delta \cos \phi - \cos \delta \sin \phi \sin \omega). \tag{34}$$

The value of K is slightly smaller than 1 when $\beta \approx \pi/2$. The difference between the values of θ_m and θ is given by

$$\epsilon_{\delta,\phi} = \theta_m - \theta = -R\theta, \tag{35}$$

where $R = 1 - K$.

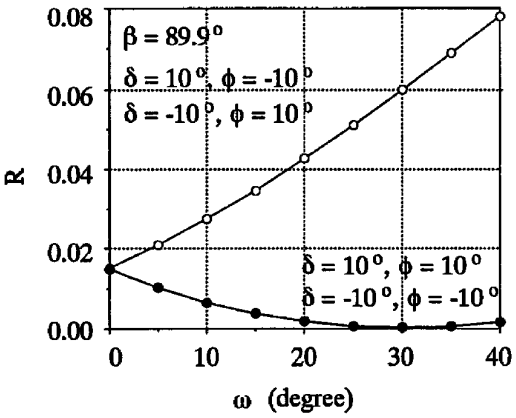

Fig. 5. Ratio R of error $\epsilon_{\delta,\phi}$ versus incident angle ω.

4. Error Analysis

First, we examine how much the measurement error $\epsilon_{\delta,\phi}$ is in the nonideal configuration. The error $\epsilon_{\delta,\phi}$ is proportional to the rotation angles as shown by Eq. (35), and the ratio R is a significant value. The ratio R is a function of angles δ and ϕ as well as incident angle ω as shown in Eq. (34). Figure 5 shows the ratio R versus the incident angle ω for $|\delta| = 10°$, $|\phi| = 10°$, and $\beta = 89.9°$. We obtain two different curves that are related to signs of angles δ and ϕ. This reason can be found in the last term in Eq. (34). When the signs of angles δ and ϕ are the same, the last term in Eq. (34) becomes small and ratio R is always less than 0.02. When the signs of angles δ and ϕ are different, ratio R increases for a large angle ω. When angle ω is smaller than 20°, R is smaller than 0.04. It is clear that we should decrease incident angle ω to decrease ratio R. Figure 6 shows that ratio R versus angle δ for $\phi = \pm 10°$, 5°, $\omega = 10°$, and $\beta = 89.9°$. The value of R decreases greatly as angle δ decreases, although R is not decreased noticeably by small angle ϕ. In the experiments it is difficult to eliminate small angle ϕ, but small angle δ is easily adjusted to within ±2°. As shown in Fig. 6, when angle δ is between −2° and 2°, the ratio error R is less than 0.005 regardless of the existence of small

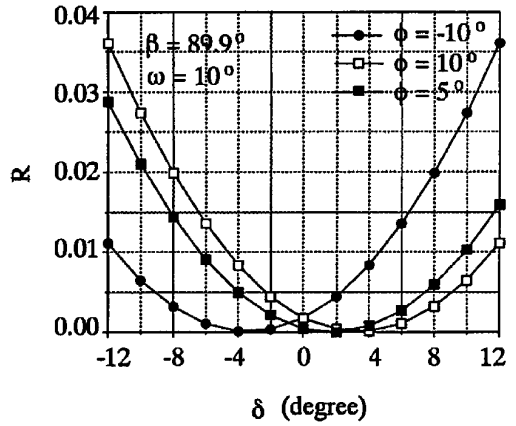

Fig. 6. Ratio R of error $\epsilon_{\delta,\phi}$ versus small inclination angle δ.

angle ϕ. It is important to adjust inclination angle δ to be small to decrease the error ratio.

Next we consider a random error ϵ_α in the measurement of θ caused by the random error in the measurement of phase differences α_0 and α. From Eqs. (2) and (31), Eq. (10) is rewritten as

$$\theta = S(\alpha - \alpha_0)/4\pi z_0. \tag{36}$$

This equation is better for experiments than Eq. (10) because values S and z_0 can be directly adjusted in the experiments. A standard deviation of ϵ_α is given by

$$\sigma_\theta = \left[\left(\frac{\partial\theta}{\partial\alpha}\right)^2 {\sigma_\alpha}^2 + \left(\frac{\partial\theta}{\partial\alpha_0}\right)^2 {\sigma_{\alpha_0}}^2\right]^{1/2}, \tag{37}$$

where σ_α and σ_{α_0} are standard deviations of α and α_0, respectively. Usually the random error in measurement of the phase difference α_0 is the same as that of phase difference α. This means that $\sigma_\alpha = \sigma_{\alpha_0} = \sigma$. From Eq. (36), Eq. (37) reduces to

$$\sigma_\theta = S\sqrt{2}\sigma/4\pi z_0 = \sqrt{2}\sigma/S_e, \tag{38}$$

where S_e is the sensitivity at $\theta = 0$ given by Eq. (11). To decrease the standard deviation σ_θ, we decrease σ or increase the value of z_0, although the value of S is determined by the structure of the interferometer. The value of z_0 can be easily changed by moving a detection point. The value of σ can be decreased by using a feedback control system to eliminate fluctuations of the phases caused by mechanical vibrations.

There are two error sources in the method. One is from a nonideal configuration of the setup, that is, $\delta \neq 0$, $\phi \neq 0$, as given by Eq. (35). Another is from the measurement error of the phase difference, α and α_0. Hence the error in the measurement of small rotation angle θ is

$$\epsilon(\theta) = \epsilon_{\delta,\phi} + \epsilon_\alpha. \tag{39}$$

5. Experimental Setup

Figure 7 shows an experimental setup for measuring rotation angle θ of the optical surface. A Twyman–Green-type interferometer is used to generate a parallel interference pattern whose period is S. Mirror 2 in the Twyman–Green-type interferometer is adjusted so that the two collimated laser beams reflected by mirrors 1 and 2, respectively, intersect each other at angle γ. The wavelength λ of light emitted from the laser diode is 780 nm. Angle γ is 4.9 arcmin, and space period S is 550 μm. The diameter of the two laser beams is ~4 mm. Because angle γ is very small, the overlap length of the two laser beams or the length of the parallel interference pattern is a few meters. Incident angle ω of the equiphase plane onto the optical surface is 10°.

Experimentally a plane on which the experimental setup is placed is regarded as plane P. The optical surface is a flat mirror that rotates around the y axis perpendicular to plane P. If we remove the optical surface, the two beams from the beam-splitter cube separate at a position far from the optical surface, and we observe two spots on a plane perpendicular to plane P. The distance between the centers of these two spots gives us a value of angle γ. The distance between the centers of the spots along a line perpendicular to plane P gives us a value of the misalignment angle δ. We can adjust angles γ and δ by observing the positions of the two beams.

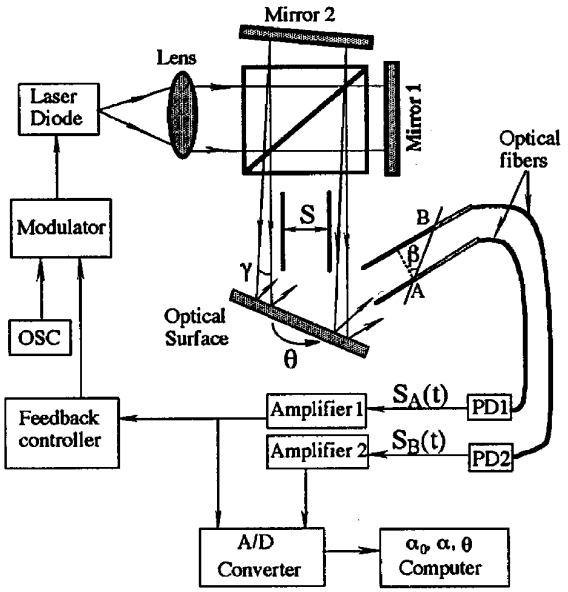

Fig. 7. Experimental setup.

Because distance d_0 between the two detection points, A and B, is less than space S, a pair of optical fibers is used to detect the interference signals at two points where the two fibers stick together. The outside diameters of the fibers are ~1 mm, and their core diameters are 50 μm. Before rotation of the optical surface, optical fibers are set along the propagation direction of the reflected laser beams to receive the light at points A and B. The value of z_0 corresponds to the distance between points A and B along the optical fibers, and the values of x_0 and y_0 correspond to the distance along the x and y axes, respectively, between the two optical fibers. Angle β is determined by the values of x_0 and z_0. The values of x_0 and y_0 are 225 μm and 2 mm, respectively. The value of z_0 can be changed. The use of the optical fibers makes it very easy to move the detection points.

A sinusoidal phase-modulating laser-diode interferometer is used to measure the phase of the equiphase plane.[9] The injection current of the laser diode is modulated with a sinusoidal wave signal $a \cos \omega_c t$ for generating a sinusoidal phase-modulated interference signal. Two interference signals, $S_A(t)$ and $S_B(t)$, are detected at points A and B in the reflected parallel interference pattern. The time-varying components of the signals at the two points are written as

$$S_A(t) = \cos(z \cos \omega_c t + \alpha_A), \tag{40}$$

$$S_B(t) = \cos(z \cos \omega_c t + \alpha_B), \tag{41}$$

where z is proportional to amplitude a of the injection

current and the optical path difference between the beams that make up the interference pattern. Two optical fibers are connected with two photodiodes, 1 and 2. Interference signals $S_A(t)$ and $S_B(t)$ are sent into a computer through an A/D converter.

Phases α_A and α_B are measured from the interference signals with the technique of a sinusoidal phase-modulating interferometer.[9] The phase difference α_0 is obtained from α_A and α_B. When the object rotates by angle θ, the phase difference α is also obtained. However, there are fluctuations in the phase of the interference signal caused by external mechanical vibrations. If we use a feedback control system in the interferometer, the fluctuations in the phase of the interference signal are depressed.[10,11] A feedback signal $\sin \alpha_A$ is produced from signal $S_A(t)$ in the feedback controller. The feedback system controls the injection current of the laser diode so that a condition of $\sin \alpha_A = 0$ is kept against the phase fluctuations. The random errors in the measurement of phase differences α_0, α are greatly decreased. A standard deviation σ of the phase differences is calculated by measuring them several times. Experimental results show that σ can be decreased from 0.1 rad to 2 mrad by using the feedback control system.

6. Experimental Results

Experiments were performed with the experimental setup in Fig. 7. In the experiments the related parameters were adjusted to $S = 550$ μm, $\omega \approx 10°$, and $\beta = 89.9°$, which were obtained at $z_0 = 120$ mm, $x_0 = 225$ μm. In the condition of $x_0 = S/2$, phase difference α_0 was equal to π. Sensitivity S_e given by Eq. (11) is 17 mrad/arcsec for small rotation angles. Angles ϕ and θ could be measured with an autocollimator.

First, we investigated error $\epsilon(\theta)$ given by Eq. (39). Figure 8 shows the experimental results and the theoretical curve of $\epsilon_{\delta,\phi}$ given by Eq. (35). Inclination angle ϕ was 5°. Inclination angle δ of the equiphase plane was adjusted from −6° to 20° at intervals of ~3°. We rotated the optical surface by −30 arcsec, measuring the rotation angle with an autocollimator. The rotation angle was measured from Eq. (36) for different values of the angle δ, and we obtained the value of $\epsilon(\theta)$, which was the difference

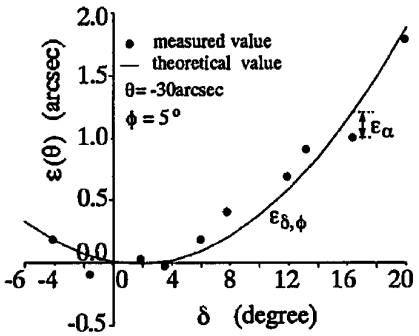

Fig. 8. Error $\epsilon(\theta)$ of the rotation angles measured at different values of δ.

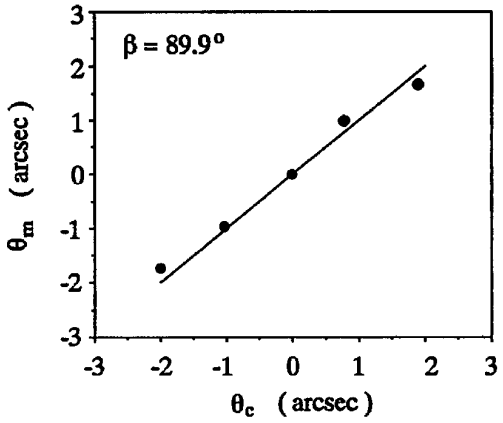

Fig. 9. Rotation angles measured within ±2 arcsec at $\beta = 89.9°$ and $\alpha_0 = \pi$.

between the measured value θ_m and the actual value of −30 arcsec. The standard deviation σ_θ of the random error ϵ_α given by Eq. (38) is 0.2 arcsec at $\sigma = 2$ mrad. The measured values agree with the theoretical values of $\epsilon_{\delta,\phi}$ to within 0.2 arcsec. Because angle δ can be easily adjusted to be within ±2°, the accuracy of 0.2 arcsec is achieved in the measurement.

Second, the small rotation angles of the optical surface were measured within ±2 arcsec at intervals of 1 arcsec in the condition that δ was within ±2° and ϕ was less than 5°. The measurement result at $\beta = 89.9°$ is shown in Fig. 9. Angle θ_c is a measured value with an autocollimator, and θ_m is the measured value by our method. The black dot at $\theta_c = 0$ or $\theta_m = 0$ indicates the initial position of the optical surface. From the experimental result, we see that the error in the measurement was within ±0.2 arcsec that arises from error ϵ_α. Figure 10 shows another measurement result when the value of z_0 was changed to 60 mm, that is, $\beta = 89.8°$. The error in the measurement increased by two, because z_0 was decreased by one half. The measurement results agree well with the theoretical results given by Eq. (38).

Figure 11 shows the values of $\epsilon(\theta) = \theta_m - \theta_c$ for the small rotation angles measured within ±30 arcsec at intervals of 5 arcsec in the condition that δ and ϕ were

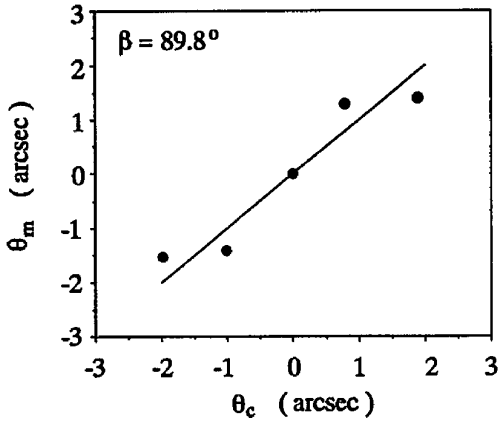

Fig. 10. Rotation angles measured within ±2 arcsec at $\beta = 89.8°$ and $\alpha_0 = \pi$.

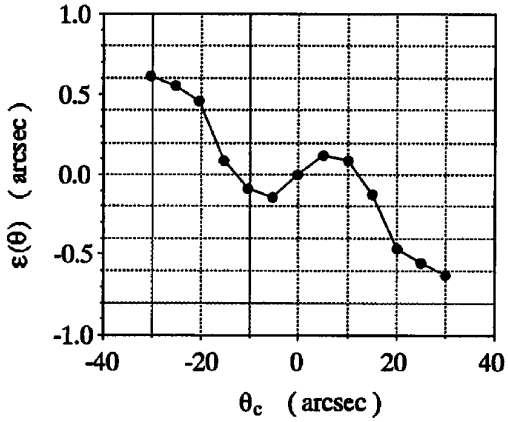

Fig. 11. Error $\epsilon(\theta)$ of the rotation angles measured within ± 30 arcsec at $\beta = 89.9°$ and $\alpha_0 = \pi$.

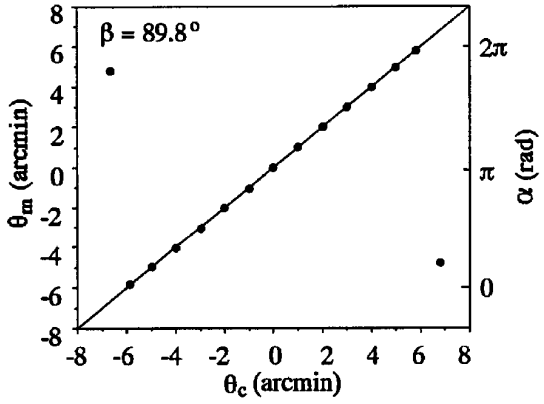

Fig. 13. Measurement range obtained at $\beta = 89.8°$ and $\alpha_0 = \pi$.

larger angles. In the results the error is approximately -0.6 arcsec at $\theta_c = 30$ arcsec. This means that error $\epsilon_{\delta,\phi}$ becomes a large value for a larger rotation angle as given by Eq. (35). From Eq. (39) $\epsilon_{\delta,\phi}$ in the measurement of the 30-arcsec rotation angle is between -0.8 and -0.4 arcsec, that is, value R is between 0.013 and 0.027. From Fig. 6 we estimate that the values of angle δ and ϕ are near $\pm 8°$, and the δ sign was different from the ϕ sign. The experimental results show that the adjustment of angle δ is important in the method. The error in the measurement of small rotation angles is provided mainly by error ϵ_α. Error $\epsilon_{\delta,\phi}$ becomes larger than error ϵ_α for large rotation angles if angle δ is not small. If angle δ is within $\pm 2°$, error $\epsilon_{\delta,\phi}$ can be ignored.

Finally we investigated the measurement range. The rotation angles were measured at intervals of 1 arcmin as shown in Fig. 12. The measurement range of θ_m is limited by the measurement range of α, which is from 2π to 0. The measured value of α corresponding to the value of θ_m is also shown in Fig. 12. The measurement range of θ_m is found by the fact that the value of α jumps over 2π for large rotation angles. These α jumps were observed as the measured values that are not on the linear line as shown in Fig. 12. When $z_0 = 120$ mm and $x_0 = 225$ μm or $\beta = 89.9°$, the measurement range was approximately ± 3 arcmin. Figure 13 shows the results at $z_0 = 60$ mm and $x_0 = 225$ μm or $\beta = 89.8°$. The measurement range was approximately ± 6 arcmin. These measurement ranges obtained from the experiments show good agreement with the theoretical ones given by Eq. (14). The measurement range is wider when angle β is not closer to $\pi/2$ or z_0 is shorter. These results confirm the limitation on the rotation of the surface between measurements. The system measurements range could be greatly increased with multiple measurements.

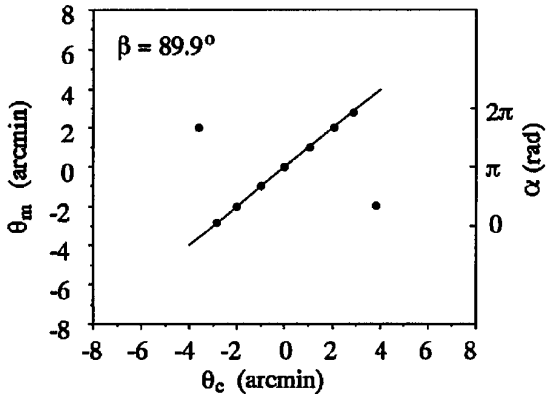

Fig. 12. Measurement range obtained at $\beta = 89.9°$ and $\alpha_0 = \pi$.

7. Conclusions

A method for measuring rotation angles by using a parallel interference pattern has been described. The principle shows that the method is suitable for measuring small rotation angles. Using the concept of the equiphase planes, we analyzed measurement error $\epsilon_{\delta,\phi}$ caused by the nonideal configuration where the equiphase planes and the optical surface are not parallel to the rotation axis of the optical surface and are inclined by angles δ and ϕ, respectively. The value of error $\epsilon_{\delta,\phi}$ is proportional to rotational angle θ, and error $\epsilon_{\delta,\phi}$ can be ignored when angle δ is within $\pm 2°$. The adjustment of δ is very important in the method. For small rotation angles of less than ~ 10 arcsec, measurement error ϵ_α that is caused by the random error in the measurement of the phase difference, α and α_0, is dominant. The standard deviations of these phase measurements is 2 mrad. These small standard deviations are obtained by using a sinusoidal phase-modulating laser-diode interferometer with the feedback control system to eliminate fluctuations in the phase of the interference signal. The sensitivity S_e at $\beta = 89.9°$ and $\alpha_0 = \pi$ is 17 mrad/arcsec for small rotation angles. Then the standard deviation of ϵ_α is 0.2 arcsec, and a measurement accuracy of 0.2 arcsec is achieved for small rotation angles. The method as demonstrated has a high spatial resolution of 0.55 mm, which is the period of the parallel interference pattern. The measurement range depends on the value of the β angle. The range is ± 6 arcmin at a β angle of 89.8°. The experimental results agree well with the theoretical

results about the measurement errors and the measurement range.

The method is very suitable for such applications as the noncontact monitor of surface tilt that keeps changing with time. In addition to a small measurement area we have the advantage that the period of the interference pattern does not change after the surface rotation. This could allow us to measure the rotation angle repeatedly and obtain a larger measurement range for the system. Then the α phase goes beyond 2π or 0, and the individual measurement must be interpreted by using a phase-unwrapping technique. We will study a larger measurement range with the method in the near future.

References

1. P. S. Huang, S. Kiyono, and O. Kamada, "Angle measurement based on the internal-reflection effect: a new method," Appl. Opt. **31,** 6047–6055 (1992).
2. B. P. Singh, K. Varadan, and V. T. Chitnis, "Measurement of small angular displacement by a modified moire technique," Opt. Eng. **31,** 2665–2667 (1992).
3. D. Malacara and O. Harris, "Interferometric measurement of angles," Appl. Opt. **9,** 1630–1633 (1970).
4. G. D. Chapman, "Interferometric angular measurement," Appl. Opt. **13,** 1646–1651 (1974).
5. P. Shi and E. Stijns, "New optical method for measuring small-angle rotations," Appl. Opt. **27,** 4342–4344 (1988).
6. T. Takano and S. Yonehara, "Basic investigations on an angle measurement system using a laser," IEEE Trans. Aerosp. Electron. Syst. **26,** 657–662 (1990).
7. P. Shi and E. Stijns, "Improving the linearity of the Michelson interferometric angular measurement by a parameter compensation method," Appl. Opt. **32,** 44–51 (1993).
8. P. R. Yoder, Jr., E. R. Schlesinger, and J. L. Chickvary, "Active annular-beam laser autocollimator system," Appl. Opt. **14,** 1890–1895 (1975).
9. O. Sasaki and K. Takahashi, "Sinusoidal phase modulating interferometer using optical fibers for displacement measurement," Appl. Opt. **27,** 4139–4142 (1988).
10. O. Sasaki, K. Takahashi, and T. Suzuki, "Sinusoidal phase modulating laser diode interferometer with a feedback control system to eliminate external disturbance," Opt. Eng. **29,** 1511–1515 (1990).
11. O. Sasaki, H. Sasazaki, and T. Suzuki, "Two-wavelength sinusoidal phase/modulating laser-diode interferometer insensitive to external disturbances," Appl. Opt. **30,** 4040–4045 (1991).